

# Agent-Based Modeling of Phagocytosis: Immune Response Simulations

Emilien Biré

2025

## Abstract

This paper presents an agent-based modeling framework to simulate phagocytosis, a critical process in the non-specific immune response, focusing on interactions between phagocytes and bacterial populations. The model incorporates biologically inspired rules to govern agent behaviors, enabling both computational exploration of infection dynamics and analytical derivation of conditions for successful infection control. By leveraging GPU-accelerated computations, the framework supports large-scale simulations in hexagonal grid environments with high agent density. Key findings identify parameter thresholds—such as phagocyte spawn rates  $r$ , infection detection thresholds  $d_{max}$ , and environment size  $L$ —that determine whether bacteria are eradicated, persist, or reach equilibrium with phagocytes. These results highlight the importance of early immune detection and phagocyte recruitment efficiency in infection outcomes. The study bridges computational modeling with mathematical analysis, offering scalable tools and theoretical insights for studying immune responses and related biological systems.

## 1 Introduction

The immune system's ability to combat infections relies on complex spatial and temporal interactions between host cells and pathogens. Agent-based modeling (ABM) provides a powerful approach to simulate such systems, capturing emergent behaviors arising from individual agent interactions. While prior studies have explored immune dynamics using ABMs, few integrate analytical rigor with scalable computational frameworks to dissect the mechanistic drivers of infection outcomes.

This work develops an ABM to investigate phagocytosis, a fundamental immune process where phagocytes detect, engulf, and eliminate bacteria. The model simplifies biological complexity into discrete rules: bacteria proliferate or migrate based on local phagocyte density, while phagocytes navigate chemotactic gradients to locate and neutralize pathogens. A hexagonal grid environment enables spatially realistic simulations, with GPU acceleration facilitating efficient computation of gradient fields and agent movements across large scales.

Beyond simulations, the study derives mathematical conditions for infection control, linking parameters like phagocyte recruitment rates and bacterial spread dynamics to three possible outcomes: bacterial dominance, phagocyte success, or equilibrium. These analytical insights are validated against simulations, revealing how early immune detection and phagocyte deployment thresholds dictate infection trajectories. By combining computational scalability, mathematical formalism, and biological intuition, this framework advances the study of immune responses and offers a foundation for exploring broader applications.

## 2 Related Work

### 2.1 Immune Response and Phagocytosis

The study of immune responses, including phagocytosis and chemotaxis, is fundamental for understanding infection dynamics. Visualization techniques are pivotal in this domain, as they enable researchers to observe cellular interactions in real time. The work by [1] provides a comprehensive review of advanced imaging methods, such as light and electron microscopy, including super-resolution techniques, to visualize host-pathogen interactions. The authors emphasize the importance of selecting appropriate cell culture systems (e.g., immortalized vs. primary cells) and integrating multiple imaging modalities to capture spatial and temporal details of bacterial colonization, invasion, and host responses. Quality controls like TEER and viability assays are also highlighted as critical for ensuring experimental validity.

## 2.2 Models for Infection Reaction and Immune Response

### 2.2.1 Agent-Based Models (ABMs)

Agent-based modeling has emerged as a powerful tool for simulating immune reactions to infections due to its ability to capture cellular heterogeneity and spatial dynamics. For instance, [2] develops an ABM to simulate the autoimmune response in type 1 diabetes, focusing on interactions between CD8+ T cells and Beta cells in non-obese diabetic (NOD) mice. The model reveals how basement membrane strength influences disease progression and demonstrates that Beta cell regeneration can exacerbate inflammation due to epitope spreading.

Similarly, [3] synthesizes recent advances in ABMs for microbial ecosystems, showcasing their utility in studying gene regulation, motility, and biofilm formation. The authors highlight ABMs' predictive power in replicating experimental findings and guiding synthetic circuit design, while also addressing computational challenges in large-scale simulations.

### 2.2.2 Mathematical Models

Mathematical approaches complement ABMs by providing a framework for understanding disease spread at the population level. The dynamic network model by [4] extends classical SIR dynamics by incorporating individual-level interactions and spatial heterogeneity. The study demonstrates that disease spread depends on both infectivity and recovery times, with spatial heterogeneities in susceptibility either amplifying or suppressing transmission. A scaling theory is introduced to predict epidemic dynamics across diverse network structures.

### 2.2.3 Simulation Tools

Several tools have been developed to facilitate ABM implementation. The Basic Immune Simulator (BIS) [5] is an ABM designed to study interactions between innate and adaptive immunity. It simulates immune responses across three virtual zones (tissue, lymphoid tissue, and circulation) and identifies three outcome patterns: immune win, immune loss, and immune hyper-response. The model underscores the critical role of dendritic cells in determining response efficacy.

Another tool, MiStImm [6], focuses on self-nonself discrimination in adaptive immunity. It compares the Conventional Role of Self (CRS) model with the Enhanced Role of Self (ERS) model, demonstrating that the latter avoids autoimmune reactions despite enhanced TCR-MHC interactions. The tool also visualizes immune memory development and aligns with clinical observations in immunotherapy.

### 2.2.4 Integration with Clinical Data and Machine Learning

Validating simulations with clinical data is essential for ensuring their relevance. [7] couples a spatial ABM with a whole-patient Quantitative Systems Pharmacology (QSP) model to study tumor growth and immunotherapy response. The hybrid model captures spatial heterogeneity in the tumor microenvironment and identifies T-cell hotspots, with results validated against digital pathology data for triple-negative breast cancer.

In another study, [8] simulates the hepatic inflammatory response (HIR) to *Salmonella* infection, incorporating 21 cell types and cytokines. The model reproduces four dynamic HIR patterns (healing, persistent infection, hyperinflammation, and organ dysfunction) and highlights biomarkers like HMGB-1 and IL-10:TNF- $\alpha$  ratios as predictors of outcomes.

Machine learning techniques are increasingly used to enhance ABMs. For example, [9] employs random forest regression and neural networks to identify key parameters (e.g., glucose concentration, growth rate) influencing microbial population growth. The metamodel achieves high accuracy in predicting logistic growth parameters, significantly reducing computational costs.

### 2.2.5 Discrete and Grid-Based Simulations

Discrete models, particularly grid-based simulations, offer a balance between simplicity and scalability. [10] introduces NetBioDyn, an intuitive ABM software for modeling biological systems without requiring programming skills. Its pedagogical utility is demonstrated through case studies like predator-prey dynamics and blood coagulation, though the tool has limitations in entity shape flexibility.

The hexagonal grid model by [11] simulates influenza viral dynamics in airway epithelial cells, capturing transitions between healthy, infected, secreting, and dead states. The model is calibrated using experimental data and provides insights into viral replication and diffusion, with future extensions proposed to include cell-type heterogeneity.

## 2.3 Our contribution

This work aims to build the following:

- A new ABM for innate immune response to infection with simple biological-inspired rules and parameters.
- Mathematical foundations for characterizing and interpreting the results of numerical simulations.
- GPU-accelerated grid calculations for faster and scalable simulations, leveraging the PyTorch framework.

### 3 Model Description

#### 3.1 Environment

The environment is a fixed hexagonal grid of radius  $L$ . The coordinate system used consists of the base  $(\vec{q}, \vec{r})$  pictured in Fig. 1.

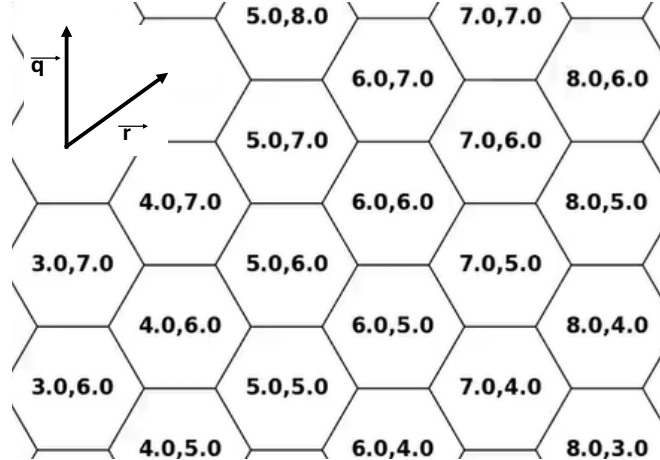


Figure 1: Visualization of the grid used for the ABM. It consists of regular hexagons in with coordinates in the base  $(\vec{q}, \vec{r})$

We introduce the hexagonal distance between two tiles in axial coordinates  $(q_1, r_1)$  and  $(q_2, r_2)$ :

$$d_{\text{hex}}(q_1, r_1, q_2, r_2) = \frac{|q_1 - q_2| + |r_1 - r_2| + |(q_1 + r_1) - (q_2 + r_2)|}{2}. \quad (1)$$

**Weight Function** During an infection, bacteria release proteins named *chemotaxis*, that immune cells will follow. Typically, phagocytes go along the increasing gradient of concentration of such proteins. We decide to model that concentration as a smooth decreasing function of the distance from the bacteria responsible for the release of chemotaxis. This *weight function* is thus defined as:

$$w_{q_c, r_c}(q, r) = \exp\left(-\frac{d_{\text{hex}}(q, r, q_c, r_c)}{2}\right), \quad (2)$$

with  $(q_c, r_c)$  being the coordinate of the bacterium responsible for the gradient. For the following, we consider that a similar weight function is used to model the awareness of phagocytes positions from one another.

**Gradients** Using the previous weight function, we can define the total gradient field, which is given by:

$$G_I(q, r) = \sum_{(q_c, r_c) \in I} w_{q_c, r_c}(q, r), \quad (3)$$

for  $I$  being either  $B$  (set of coordinates of the bacteria) or  $P$  (sets of coordinates of phagocytes). Fig. 2 shows an example of such a gradient with a few bacteria in the environment.

Since those gradients are expensive to compute, one would prefer relying on dense grids on which 2D convolution with an exponential kernel could be performed. We thus define the kernel:

$$k(q, r) = w_{0,0}(q, r),$$

with  $k \in \mathbb{R}^{L \times L}$ , and dense binary grids:

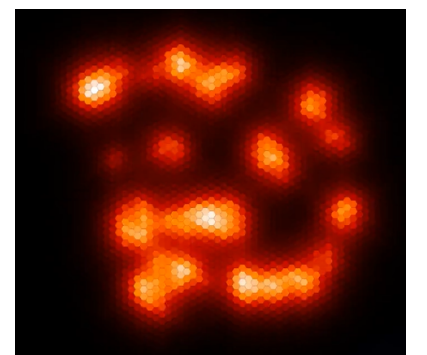
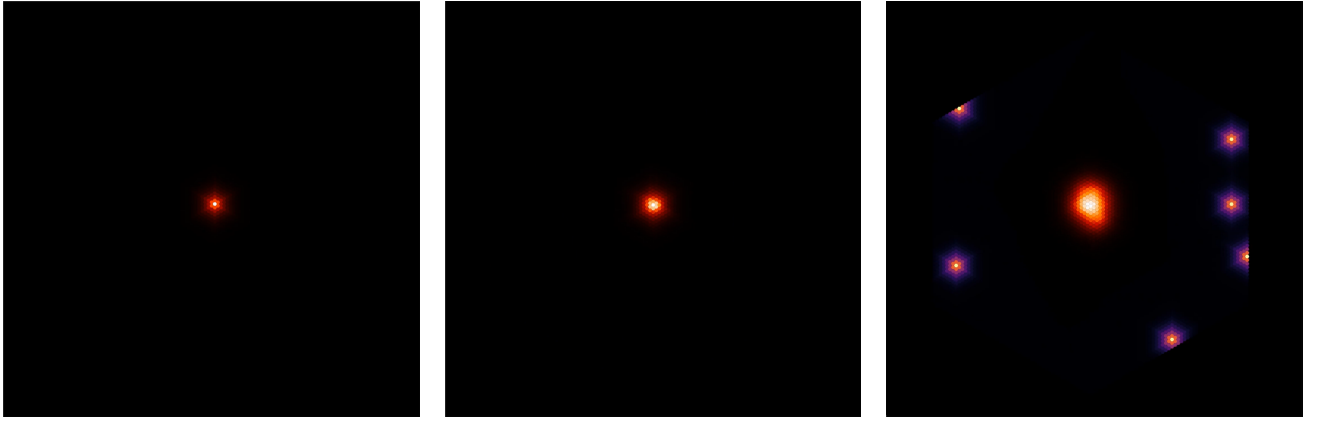


Figure 2:  $G_I(\cdot, \cdot)$



(a) Start                          (b) After a few time steps                          (c) When the first phagocytes appear

Figure 3: The beginning of a simulation until the first phagocytes appear:  $\frac{N_b}{N_p} \geq d_{\max}$ .

$$D_B(q, r) = 1 \text{ if } (q, r) \in B, \text{ else } 0,$$

$$D_P(q, r) = 1 \text{ if } (q, r) \in P, \text{ else } 0,$$

with  $D_I \in R^{2L \times 2L}$ , being the environment padded with 0 for  $L/2$  rows and columns on each side of the grid. That way, we get:

$$G_I(q, r) = (D_I * k)(q, r), \quad (4)$$

At each generation, we can compute that convolution with GPU acceleration using PyTorch framework and the built-in 2D-convolution function in the Neural Network module. We can then access the value of the gradient field at each position of the environment.

Initially, the environment starts with a bacteria at the center and no phagocytes. Phagocytes are introduced based on two parameters: the spawn rate  $r$  and the maximum density threshold  $d_{\max}$ . At each time step, we check the condition:

$$\frac{N_b}{N_p} \geq d_{\max}$$

If fulfilled, new phagocytes are spawned at a rate of  $r$  per generation. These phagocytes appear randomly along the contour of the environment. Fig. 3 show the first time steps of a simulation, with bacteria represented by the induced gradient (white to red) as for the phagocytes (white to purple).

### 3.2 Agents

#### Bacteria:

- Die if engulfed.
- Otherwise, with  $p_{split} = \frac{n_{free}}{n_{tot}+1}$  with  $n_{tot}$  being the total number of neighbors and  $n_{free}$  being the number of vacant neighbor spaces: proliferate with probability  $p_{split}$

#### Phagocytes:

- Die if more than 5/6 bacteria neighbors.
- Engulf all bacteria neighbors.
- Otherwise, move to  $(q, r) = \arg \max_{(q, r) \in Neighbors} \left\{ \frac{G_B(q, r)}{G_P(q, r)} \right\}$ .

## 4 Preliminaries

### 4.1 Hexagonal grid

**Lemma 4.1.** *In a hexagonal dense grid of radius  $R$ , there are*

$$N = 3R(R + 1) + 1 \quad (5)$$

unit hexagons, and

$$R \approx \sqrt{\frac{N}{3}} \quad (6)$$

*Proof.* Equation 5 can be found by recursion: We start at  $R = 0$  with a single cell  $N_0 = 1$ . Then for  $R \geq 1$ , we add all the neighbors of the previous ring:

$$N = 1 + \sum_{k=0}^R 6k = 1 + 6 \frac{R(R+1)}{2}$$

Which gives the desired Eq. 5. Equation 6 is found by rewriting Eq. 5

$$3R^2 + 3R + 1 - N = 0,$$

solving for R, and we get

$$R = \frac{1}{2} \left( \sqrt{\frac{4N}{3}} - \frac{1}{3} + 1 \right) \approx \sqrt{\frac{N}{3}}$$

□

## 4.2 Evolution of bacteria

We start from a single bacteria and we let it proliferate freely. The natural expansion shape is uniform around the starting position.

**Lemma 4.2.** *The evolution of the number of bacteria is given by:*

$$B(t) = \left( \frac{2\sqrt{3}}{5} t + \sqrt{B_0} \right)^2 \quad (7)$$

With  $B_0$  the initial number of bacteria and a probability of splitting  $p_{split} = \frac{n_{free}}{n_{tot}+1} = \frac{2}{7}$

*Proof.* Writing the recursion formula on  $B(t)$ :

$$B(t+1) = B(t) + p_{split} \times \delta B(t), \quad (8)$$

With  $\delta B(t)$  being the number of bacteria having at least one empty neighbor. We will first prove the following:

$$\delta B(t) = \frac{6}{\sqrt{3}(1-p_{split})} \sqrt{B(t)} \quad (9)$$

Let  $R$  be the biggest radius for which the number of edge bacteria  $\delta B(R) = 6R$  which is the number of unit hexagonal cells on the edge of a dense grid of radius  $R$ . Letting each bacteria having a probability  $p_{split}$  of splitting to an neighboring empty cell, we get  $\delta B(R+1) = p_{split}\delta B(R)$ ,  $\delta B(R+2) = p_{split}\delta B(R+1) = p_{split}^2\delta B(R)$ , ... and

$$\delta B(\bar{R}) = \sum_{i=0}^{\infty} \delta B(R+i) = 6R \sum_{i=0}^{\infty} p_{split}^i = \frac{6R}{1-p_{split}},$$

with

$$\bar{R} = \frac{\sum_{i=0}^{\infty} (R+i)\delta B(R+i)}{\sum_{i=0}^{\infty} \delta B(R+i)} = R + \frac{p_{split}}{(1-p_{split})^3} \approx R.$$

Using Eq. 6 to replace  $R$  we get the desired result for  $\delta B(t)$ .

Now let's determine  $p_{split}$ . It is defined as  $p_{split} = \frac{n_{free}}{n_{tot}+1}$ . We get  $n_{free}$  noticing that on a dense hexagonal grid:

- 6 edge cells have 3 neighbors.
- $6R - 6$  cells have 2 neighbors.

As  $R$  increases,  $n_{free} \approx 2$ , thus we use as a first approximation  $p_{split} = \frac{2}{7}$ .

By putting everything together in Eq. 8:

$$B(t+1) = B(t) + \frac{6p_{split}}{\sqrt{3}(1-p_{split})} \sqrt{B(t)} = \frac{12}{5\sqrt{3}} \sqrt{B(t)} \quad (10)$$

solving Eq. 10 as a temporal ODE making the assumption that the states from one generation to the next are close:

$$\frac{\Delta B}{2\sqrt{B}} = \frac{2\sqrt{3}}{5} \Delta t \quad (11)$$

which gives us the desired formula. □

### 4.3 Evolution of phagocytes

When the number  $d_{max}$  of bacteria is reached, the first phagocytes are spawned at a rate  $r$  from a random point at a distance  $L$  to the origin of the infection, keeping the ratio  $\frac{B(t)}{P(t)} < d_{max}$ .

**Lemma 4.3.** *The number of phagocytes at a time step  $t$  is given by:*

$$P(t) = \min(rt, rn), \quad (12)$$

With  $n = \frac{B(t)}{rd_{max}}$

*Proof.* We recall the definition of  $d_{max}$ , and introduce  $d(t) = \frac{B(t)}{P(t)+1}$ . Let us give remarks:

- At  $t_0$  the first time  $d(t_0) \geq d_{max}$ ,  $P(\cdot)$  is increased by  $r$ , and  $d(t_0 + 1) = \frac{B(t_0)}{r+1}$ . Then,  $d(t_0)$  would possibly go back below  $d_{max}$ , and then we would have to wait again until  $t_1$  such that  $d(t_1) \geq d_{max}$  again.
- $P(\cdot)$  will be increased by  $r$  every time  $d(\cdot)$  goes above  $d_{max}$  again. That is, after  $t_n$ ,  $P(t_n) = nr$ .

With these remarks, we can say that the number of phagocytes will "chase" the number of bacteria, at a rate given by

$$nrd_{max} = B(t), \quad (13)$$

giving us the equation for  $n$ . However, the number of phagocytes cannot increase more than  $r$  per timestep, thus we are bounded by  $P(t) = rt$ . We finally get the desired formula, following the second remark and Eq. 13.  $\square$

### 4.4 Critical time

**Lemma 4.4.** *The critical time  $\tilde{t}$  at which the phagocytes and bacteria encounter is given by:*

$$\tilde{t} = \max\left(\frac{5}{7}(L - \sqrt{\frac{B_0}{3}}), t_{d_{max}}\right) \quad (14)$$

*Proof.* The radius  $R(t)$  at which the agents will meet is given by:

$$R_B(t) = R_P(t) \implies \sqrt{\frac{B(t)}{3}} = L - t, \text{ for } t \geq t_{d_{max}}$$

since the "speed" of phagocytes is of 1 cell towards the bacteria each time step. We define  $t_{d_{max}}$  as the first time  $d_{max}$  bacteria infected the zone i.e. when the first phagocytes are spawned:

$$B(t_{d_{max}}) \geq d_{max} \implies t_{d_{max}} = \max\left(\frac{2(\sqrt{d_{max}} - \sqrt{B_0})}{\sqrt{3}}, 0\right)$$

Using Lemma 4.2 to replace  $B(t)$  we derive the desired formula.  $\square$

### 4.5 Results with the macro-models

We check if the evolution of the populations throughout the beginning of the simulations matches our models 4.2, 4.3 and 4.4. Fig. 4 show that our models seem to fit well our simulations with different configurations of  $L$ ,  $r$ , and  $d_{max}$ , at least until  $\tilde{t}$  is reached. We can thus use those models to derive conditions on the outcome of a simulation, with respect to initial conditions.

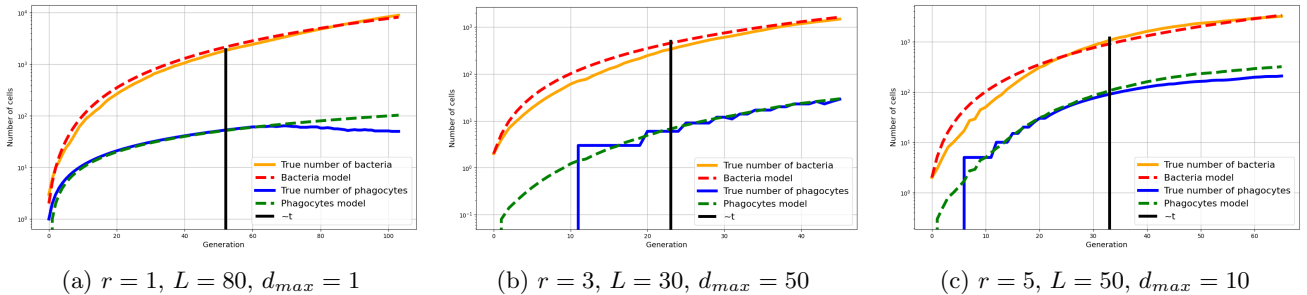


Figure 4: Evolution of populations for different starting configurations and the corresponding macro-models

## 5 Outcomes

We can classify the outcome into three possibilities :

- **Bacteria win:** they occupy all the space, preventing new phagocytes to spawn. This is the trivial result of a really low immune response: either  $d_{max}$  is too large, or the rate  $r$  is too low.
- **Phagocytes win:** there are no longer any bacteria in the environment. This is the trivial outcome of a highly effective immune response: either  $d_{max}$  is low, either the rate  $r$  is high in a large enough environment.
- **Equilibrium:** both phagocytes and bacteria are present.

### 5.1 Win of phagocytes

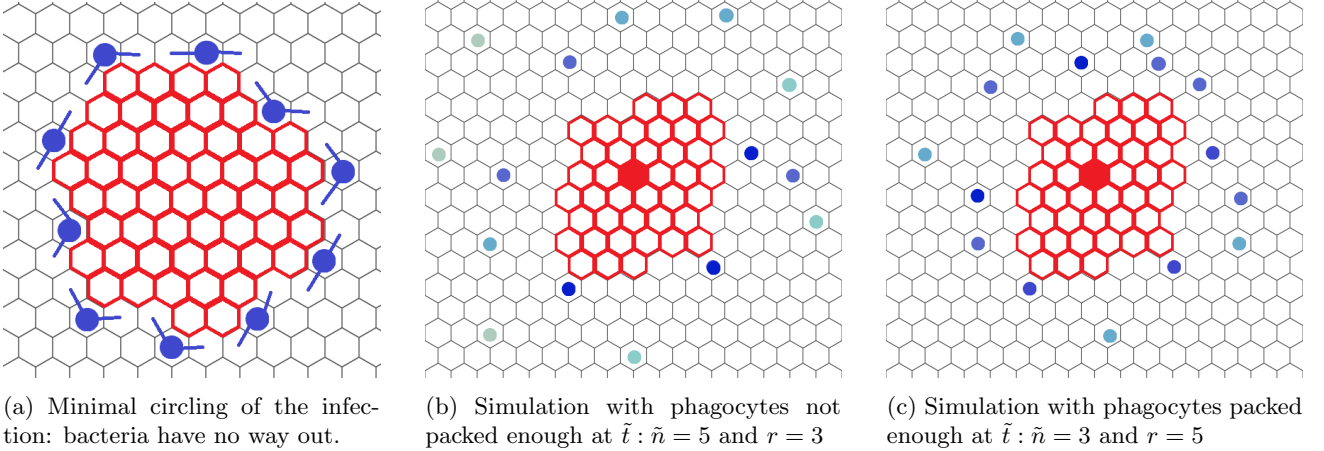


Figure 5: Illustrations of the proof of Condition 5.1. With (b) and (c), we illustrate the motivation for the formula of the discounted factor  $\gamma$ . The number of phagocytes at  $\tilde{t}$  is the same, so is  $d_{max}$ , but the rate  $r$  differs: the resulting configuration of phagocytes is either packed enough or not to enable a leakage-free circling.

**Condition 5.1.** If  $P(\tilde{t}) \geq \frac{1}{3}\delta B(\tilde{t} + 1)$  then phagocytes win. Using Lemma 4.1 and 4.2 we get:

$$-\tilde{t} - \frac{2}{3}\sqrt{6} + r \sum_{k=0}^{\tilde{t}-1} \gamma^k \geq 0 \implies \text{Phagocytes win} \quad (15)$$

$$\text{With } \gamma = \frac{\tilde{n}}{\tilde{t}} = \frac{B(\tilde{t})}{rd_{max}\tilde{t}}$$

*Proof.* We notice that a sufficient condition for a phagocytes' win would be to circle the infection cluster. For that to happen, phagocytes need to be sufficiently numerous to completely surround the bacteria without a breach, in which bacteria could spread out. That is of course if the phagocytes are "packed" enough. The minimum number necessary to circle the bacteria is a third of the number of empty cells on the edge of the infection cluster (a phagocyte "controls" its neighboring cells), as pictured in Fig. 5.

To counterbalance the latency of arrival of phagocytes, we introduce the discounted factor  $\gamma$

**Deriving  $\gamma$**  Since the parameters  $r$  and  $d_{max}$  influence the resulting density of phagocytes. Indeed, as pictured in Fig 5b and 5c, for a same number of phagocytes, the value of  $r$  and  $d_{max}$  give 2 really different configurations. The first one, too spread out, will likely not prevent the bacteria to continue expanding. However, the second one will likely lead to a controlled outcome. We can thus introduce a metric of density: phagocytes are distributed inside a doughnut of width  $L - (L - \tilde{t}) = \tilde{t}$ , on  $\tilde{n}$  concentric circles, given by Eq. 13. Finally,  $\gamma = \frac{\tilde{n}}{\tilde{t}}$ .  $\square$

**Results** Running experiments, we can plot the outcome and the iso-curve given by Condition 5.1. We report the results in Fig.6. The points below the curves for each value of  $r$  show that phagocytes controlled the infection each time. An example of such a simulation is shown in Fig. 7, where we can see the "circling" effect described in Condition 5.1, which prevents the infection from spreading.

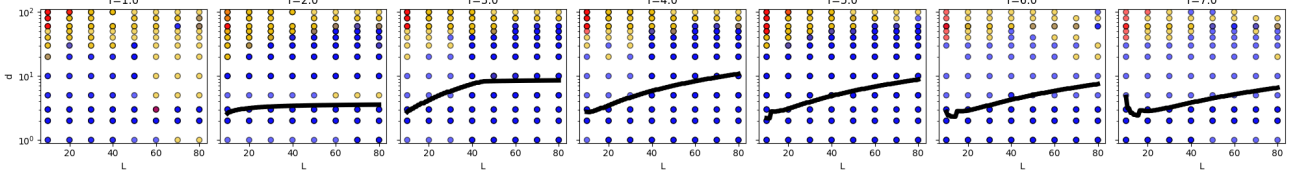


Figure 6: Simulations ran with several values of  $r, L$  and  $d_{max}$ . In black, the iso-curve below which the phagocytes are sure to win by circling the infection.

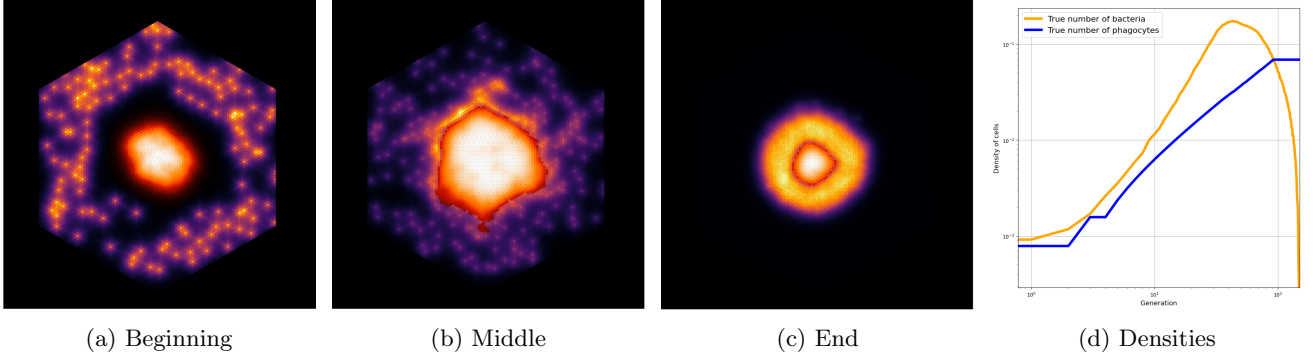


Figure 7: Simulation snapshots at different time steps in the case of a sure win of phagocytes, with  $r = 6$ ,  $L = 50$ ,  $d_{max} = 1$

## 5.2 Loss of phagocytes or equilibrium

**Condition 5.2.** If  $P_{max}(t) \leq \frac{\sqrt{3}}{2}L$  then phagocytes can't win. Using Lemma 4.3, the definition of  $d_{max}$  and Eq. (5) we get:

$$1 + 3L(L - 1) - \frac{\sqrt{3}}{2}L(d_{max} + 1) \geq 0 \implies \text{Phagocytes can't win} \quad (16)$$

*Proof.* If the maximum number of phagocytes  $P_{max}$  possible is too low, they will not be able to form a sufficiently large barrier to prevent the spread of bacteria, i.e. prevent a leakage. The minimum length of such a barrier from one end of the environment to the other is given by  $\frac{\sqrt{3}}{4}L$  using the Pythagoras theorem and the definition of  $L$ . Then, since only one bacteria is necessary to engulf 2 bacteria next to each other, the minimum number of phagocytes is brought to  $\frac{\sqrt{3}}{2}L$  for a dense barrier. The outcome will then depend on the probability that this kind of barrier occurs throughout the simulation.  $\square$

**Results** Running experiments, we can plot the outcome and the iso-curve given by Condition 5.2. We report the results on Fig. 8. Above the iso-curve, we can see that no simulations resulted in phagocyte win, and for the small environment  $L = 10$ , the outcome was even a total control of the bacteria.

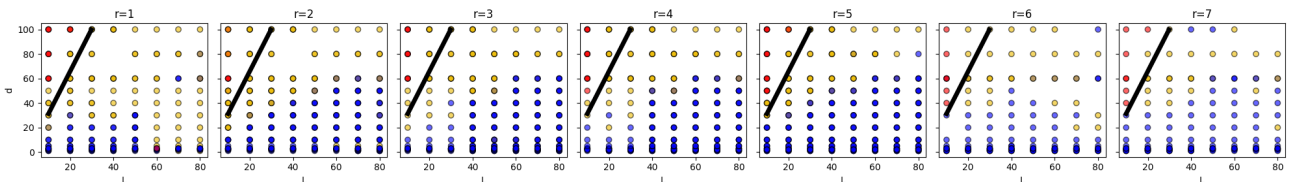


Figure 8: Simulations ran with several values of  $r, L$  and  $d_{max}$ . In black, the iso-curve above which the phagocytes can't win because their number will never reach a sufficient amount to maintain the infection.

- Fig. 9 shows an example of such a simulation. Observing the evolution of the simulation, we can see that the phagocytes aren't dense enough to prevent their death, and the bacteria had the opportunity to prevent new phagocytes from spawning by occupying the whole space.
- For larger environments ( $L > 10$  and  $d_{max} < 100$ ) it becomes less probable that it will happen, thus an equilibrium in favor of bacteria holds. That is because phagocytes have more time to re spawn, before bacteria take up the whole grid, as pictured on Fig. 10.

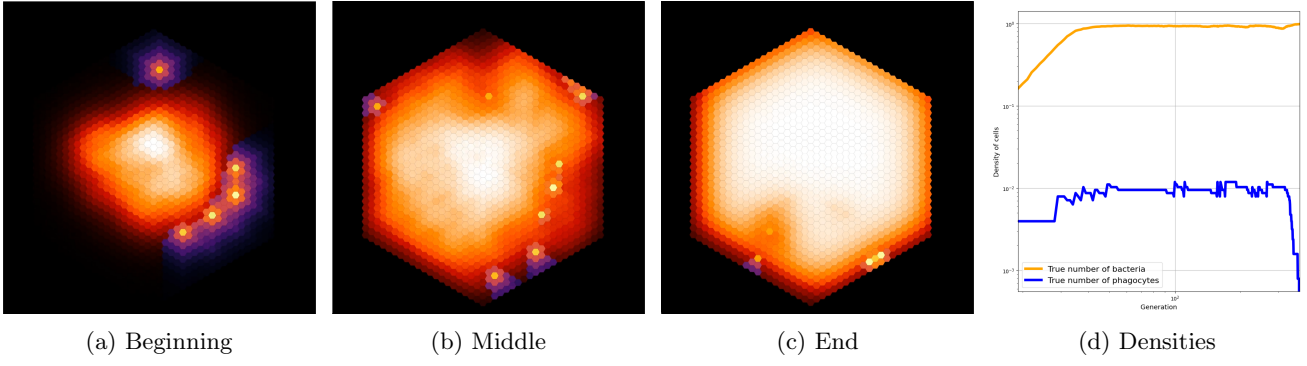


Figure 9: Simulation snapshots at different time steps in the case of a loss of phagocytes, with  $r = 5$ ,  $L = 20$ ,  $d_{max} = 100$

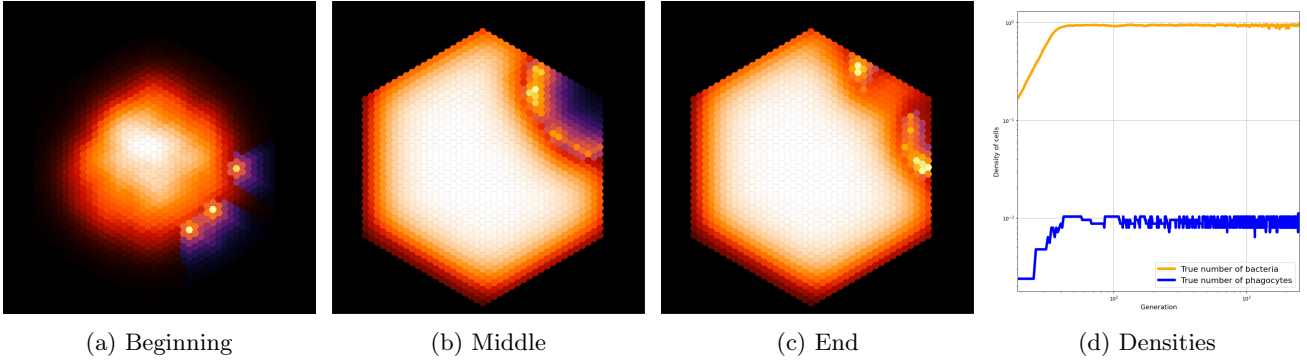


Figure 10: Simulation snapshots at different time steps in the case of an equilibrium, with  $r = 3$ ,  $L = 20$ ,  $d_{max} = 80$

### 5.3 Statistics on simulations

After exploring the results for the analytical derivations above, we can run multiple simulations for each set of parameters in a dense grid of  $r$ ,  $L$  and  $d_{max}$ . The typical ranges of our parameters are  $L \in [10, 80]$ ,  $r \in [1, 8]$ , and  $d_{max} \in [1, 100]$ . Based on the result of the simulation, we can infer statistics and probability of phagocytes' win. Fig. 11 shows the area of 95% chance of success, after training a Support Vector Machine (SVM) with a quadratic kernel:

$$K(\mathbf{x}, \mathbf{y}) = (\mathbf{x}^T \mathbf{y} + c)^2,$$

with  $\mathbf{x} = (r, L, d_{max})$  and  $\mathbf{y} = 1$ , if phagocytes won, else 0.

We can see that the area of the region increases as  $r$  increases, until  $r \geq 4$  where it stays roughly similar. That is, when  $d_{max}$  increases, the value of  $r$  no longer influences the outcome of the simulation in favor of the phagocytes. That can be interpreted as *the production of new phagocytes is not as important as the early detection of the infection, in the successful management of the latter, in a non-specific immune response*.

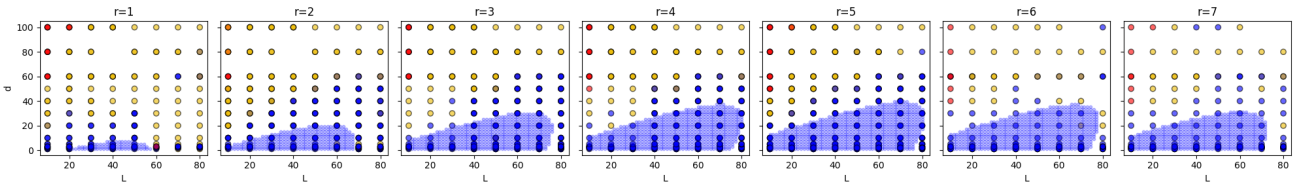


Figure 11: Simulations ran with several values of  $r, L$  and  $d_{max}$ . In light blue, the region with 95 % chance of phagocytes' win.

## 6 Conclusion and Future Work

This work demonstrates how simple interaction rules lead to emergent cooperation in an immune response model. Future work includes refining analytical approximations and exploring extensions with more sophisticated

bacterial evasion strategies, and comparing the results with clinical data and observations. The simulation framework could be further optimized to enable experiments with hundreds of thousands of cells, to check the scalability of the macro-models derived in this study. In addition, more complex mathematical modeling could be performed, introducing percolation to further assess the phase transition and characterize the *equilibrium* outcome highlighted in the experiments. One could also think of other applications, outside of biology and infectious attack modeling, such as fluid leakage or fire control.

## References

- [1] Amber J. Park, Madison A. Wright, Elyse J. Roach, and Cezar M. Khursigara. Imaging host-pathogen interactions using epithelial and bacterial cell infection models. *Journal of Cell Science*, 134(5):jcs250647, 02 2021.
- [2] M. C. Ozturk, Q. Xu, and A. Cinar. Agent-based modeling of the interaction between cd8+ t cells and beta cells in type 1 diabetes. *PLoS ONE*, 13(1):e0190349, 2018.
- [3] Karthik Nagarajan, Congjian Ni, and Ting Lu. Agent-based modeling of microbial communities. *ACS Synthetic Biology*, 11(11):3564–3574, 2022. Epub 2022 Oct 31.
- [4] Christopher A. Browne, Daniel B. Amchin, Joanna Schneider, and Sujit S. Datta. Infection percolation: A dynamic network model of disease spreading. *Frontiers in Physics*, Volume 9 - 2021, 2021.
- [5] Virginia A. Folcik, Gary C. An, and Charles G. Orosz. The basic immune simulator: An agent-based model to study the interactions between innate and adaptive immunity. *Theoretical Biology and Medical Modelling*, 4(1):39, 2007.
- [6] Csaba Kerepesi, Tibor Bakács, and Tamás Szabados. Mistimm: an agent-based simulation tool to study the self-nonself discrimination of the adaptive immune response. *Theoretical Biology and Medical Modelling*, 16(1):9, 2019.
- [7] A. Ruiz-Martinez, C. Gong, H. Wang, R. J. Sové, H. Mi, H. Kimko, et al. Simulations of tumor growth and response to immunotherapy by coupling a spatial agent-based model with a whole-patient quantitative systems pharmacology model. *PLoS Computational Biology*, 18(7):e1010254, 2022.
- [8] Zhenzhen Shi, Stephen K. Chapes, David Ben-Arieh, and Chih-Hang Wu. An agent-based model of a hepatic inflammatory response to salmonella: A computational study under a large set of experimental data. *PLoS One*, 11(8):e0161131, 2016.
- [9] Serena H. Chen, Pablo Londoño-Larrea, Andrew Stephen McGough, Amber N. Bible, Chathika Gunaratne, Pablo A. Araujo-Granda, Jennifer L. Morrell-Falvey, Debsindhu Bhownik, and Miguel Fuentes-Cabrera. Application of machine learning techniques to an agent-based model of pantoea. *Frontiers in Microbiology*, Volume 12 - 2021, 2021.
- [10] Pascal Ballet, Jérémie Rivière, Alain Pothet, Michaël Théron, Karine Pichavant, Frank Abautret, Alexandra Fronville, and Vincent Rodin. Modelling and Simulating Complex Systems in Biology: introducing Net-BioDyn. In *Multi-Agent-Based Simulations Applied to Biological and Environmental Systems*. IGI Global, February 2017.
- [11] Catherine Beauchemin, Stephanie Forrest, and Frederick T. Koster. Modeling influenza viral dynamics in tissue. In Hugues Bersini and Jorge Carneiro, editors, *Artificial Immune Systems*, pages 23–36, Berlin, Heidelberg, 2006. Springer Berlin Heidelberg.